Research Paper
J. Astron. Space Sci. 34(4), 251-256 (2017)
https://doi.org/10.5140/JASS.2017.34.4.251

JASS Journal of Astronomy and Space Sciences

Time-Varying Seismogenic Coulomb Electric Fields as a Probable Source for Pre-Earthquake Variation in the Ionospheric F2-Layer

Vitaly P. Kim[1], Valery V. Hegai[1†], Jann Yenq Liu[2], Kwangsun Ryu[3], Jong-Kyun Chung[4]

[1]Pushkov Institute of Terrestrial Magnetism, Ionosphere and Radiowave Propagation, Russian Academy of Sciences (IZMIRAN), Moscow 108841, Russia
[2]Institute of Space Science, National Central University, Taoyuan City 32001, Taiwan
[3]Satellite Technology Research Center, Korea Advanced Institute of Science and Technology, Daejeon 34141, Korea
[4]Korea Astronomy & Space Science Institute, Daejeon 34055, Korea

The electric coupling between the lithosphere and the ionosphere is examined. The electric field is considered as a time-varying irregular vertical Coulomb field presumably produced on the Earth's surface before an earthquake within its epicentral zone by some micro-processes in the lithosphere. It is shown that the Fourier component of this electric field with a frequency of 500 Hz and a horizontal scale-size of 100 km produces in the nighttime ionosphere of high and middle latitudes a transverse electric field with a magnitude of ~20 mV/m if the peak value of the amplitude of this Fourier component is just 30 V/m. The time-varying vertical Coulomb field with a frequency of 500 Hz penetrates from the ground into the ionosphere by a factor of ~7×10^5 more efficient than a time independent vertical electrostatic field of the same scale size. The transverse electric field with amplitude of 20 mV/m will cause perturbations in the nighttime F region electron density through heating the F region plasma resulting in a reduction of the downward plasma flux from the protonosphere and an excitation of acoustic gravity waves.

Keywords: earthquake, Coulomb field, ionospheric perturbation

1. INTRODUCTION

The peak ionospheric F2-layer electron density N_mF2 is subject to numerous variations and perturbations (e.g., Rishbeth 1993; Rishbeth & Mendillo 2001; Kim & Hegai 2016). One of the possible sources of N_mF2 perturbations can be strong earthquakes. Effects of earthquakes on the F region ionosphere are documented in many works (e.g. Leonard & Barnes 1965; Row 1966; Calais & Minster 1995; Ducic et al. 2003; Artru et al. 2004; Astafyeva & Afraimovich 2006; Rolland et al. 2011; Maruyama et al. 2016; Hegai et al. 2017). At the same time, Pulinets & Boyarchuk (2004) refer to numerous observations of abnormal ionospheric variations preceding earthquakes, which were reported before 2004. Since then dozens more papers devoted to this subject have been published (e.g. Liu et al. 2006; Oyama et al. 2008; Zhao et al. 2008; Liu et al. 2010; Kuo et al. 2011; Liu et al. 2011; Oyama et al. 2011; Li & Parrot 2013; Kuo et al. 2014; Daneshvar & Freund 2017; Liu et al. 2017). However, physical mechanisms that could be responsible for pre-earthquake ionospheric modification is far from been understood. In the literature, several candidates to modify the ionosphere before earthquakes have been discussed (see references in Hegai et al. 2015). One of them is the quasi-static electric field observed before some earthquakes as a perturbation in the vertical atmospheric electric field on the Earth's surface (E_z) within the earthquake's preparation zones (see references in Hegai et al. 2015). The magnitude of the observed pre-earthquake perturbations in E_z ranges between tens of V/m to 1,000 V/m. The lateral scale size of E_z perturbation region (centered at the earthquake's epicenter) can exceed 1,000 km (Hao et al. 2000). The underlying mechanism of generation

Received 25 SEP 2017 **Revised** 28 NOV 2017 **Accepted** 29 NOV 2017
†**Corresponding Author**
Tel: +7-4958-519780, E-mail: hegai@izmiran.ru
ORCID: https://orcid.org/0000-0003-0843-9096

of quasi-static electric field prior earthquakes is presently unclear. There have been suggested that it is related to the hole electric current produced by the stressed crystal rock (see references in Hegai et al. 2015). The seismogenic electric field penetrated into the ionosphere can affect the plasma distribution in the F region (Hegai et al. 1997; Pulinets & Boyarchuk 2004; Hegai et al. 2006; Kuo et al. 2011; Liu et al. 2011; Kuo et al. 2014; Hegai et al. 2015; Kelley et al. 2017). Zhang et al. (2012, 2014) reported that Detection of Electro-Magnetic Emissions Transmitted from Earthquake Regions (DEMETER) satellite observed perturbations in the ultra low frequency (ULF) / extremely low frequency (ELF) electromagnetic field in the ionosphere at 660-710 km before earthquakes over their epicentral zones. Zhang et al. (2014) found perturbations in the electrostatic waves at 15 Hz with amplitude of 1.5-16 mV/m, mostly less than 10 mV/m.

In this paper we assume that before earthquakes there can be generated time-varying perturbations in the vertical electrostatic (Coulomb) field on the Earth's surface within the earthquake's epicentral zone and study penetration of these perturbations into the ionosphere. Possible effects of the penetrated electric field on the nighttime ionospheric F2-layer are also discussed.

2. BASIC ASSUMPTIONS AND EQUATIONS

The key assumption fundamental to the present study is that before earthquakes (within their epicentral zones) there can be generated time-varying irregular perturbations in the vertical Coulomb electric field on the Earth's surface due to some mechanism operating in the lithosphere. We represent these irregular temporal variations in the vertical electric field as a Fourier series of simple harmonically related sinusoidal functions, and further consideration is convenient to make for one such a sine function. The medium is assumed to be horizontally stratified with isotropic conductivity below 90 km. Assuming the Earth's surface to be flat, we introduce cylindrical coordinates (r, φ, z) centered at a forthcoming earthquake's epicenter and with the z axis pointing vertically upward (Kim et al. 2012).

The Maxwell's equations for electromagnetic field can be written the form

$$\mathrm{div}\,\boldsymbol{E} = \rho/\varepsilon_0 \tag{1}$$

$$\mathrm{curl}\,\boldsymbol{E} = -\,\partial\boldsymbol{B}/\partial t \tag{2}$$

$$\mathrm{div}\,\boldsymbol{B} = 0 \tag{3}$$

$$c^2\mathrm{curl}\,\boldsymbol{B} = j/\varepsilon_0 + \partial\boldsymbol{E}/\partial t \tag{4}$$

$$\boldsymbol{j} = \sigma\boldsymbol{E} \tag{5}$$

where $\boldsymbol{E}$ and $\boldsymbol{B}$ are the electric and magnetic fields, respectively, ρ the electric charge density, ε_0 the vacuum permittivity, c the light velocity, $\boldsymbol{j}$ the electric current density, and σ the electrical conductivity. We'll consider only the curl-free component of the electric field (Coulomb electric field) for which above system of Eq. (1) – Eq. (5) are reduced to the equations

$$\mathrm{div}\,\boldsymbol{E} = \rho/\varepsilon_0 \tag{6}$$

$$\partial\rho/\partial \mathrm{t} + \mathrm{div}\,\boldsymbol{j} = 0 \tag{7}$$

From these equations one can finally obtain

$$\partial(\varepsilon_0\,\mathrm{div}\,\boldsymbol{E})\,/\partial t + \mathrm{div}\,\sigma\,\boldsymbol{E} = 0 \tag{8}$$

If $\boldsymbol{E} = \boldsymbol{E}(r)\,\mathrm{e}^{\mathrm{i}\omega t}$ (where ω is an angular frequency) we obtain from Eq. (8)

$$\mathrm{div}\,(\mathrm{i}\omega\varepsilon_0 + \sigma)\,\boldsymbol{E}(r) = 0 \tag{9}$$

We can introduce the ratio $s(z) = \omega\varepsilon_0/\sigma$ which describes the electric properties of the medium. If $s >> 1$ then Eq. (9) reduces to

$$\mathrm{div}\,\boldsymbol{E}(r) = 0 \tag{10}$$

that implies that the medium can be considered as a vacuum. If $s << 1$ then Eq. (9) reduces to

$$\mathrm{div}\,\sigma\boldsymbol{E}(r) = 0 \tag{11}$$

and the medium can be taken as a conductive medium. The height z_b below which the medium can be regarded as a vacuum ($s >> 1$) depends on the frequency ω and the conductivity profile. If the horizontal scale size of $\boldsymbol{E}(r)$ is much larger than z_b then for heights from 0 km to z_b, $\boldsymbol{E}$ practically does not change with z and $\boldsymbol{E}(z = 0) \approx \boldsymbol{E}(z = z_b)$. It is an important point for mapping of $\boldsymbol{E}$ into the ionosphere.

Thus, penetration of the electric field into the ionosphere is governed by Eq. (11) and

$$\boldsymbol{E}(r) = -\,\mathrm{grad}\,\Phi \tag{12}$$

where Φ is the electrostatic potential. To calculate a distribution of the electric field in the ionosphere, Eq. (11) is sufficiently to be solved within the height range between z_b and 90 km since above 90 km, the geomagnetic field lines can be taken as equipotentials because the conductivity along the geomagnetic field is high and much larger than the conductivity transverse to the geomagnetic field, i.e., the potential Φ at z = 90 km determines Φ at ionospheric heights above this level, and the electric field is perpendicular to the geomagnetic field lines. Furthermore, the ionosphere above 90 km can be thought of as a thin conductive layer with Pedersen conductivity integrated along the geomagnetic field lines Σ_p, and Eq. (11) takes the following form at z = 90 km

$$\sigma \boldsymbol{E}_z = \nabla_\perp \cdot (\Sigma_p \boldsymbol{E}_\perp) \tag{13}$$

where $\boldsymbol{E}_z = -\,\partial\Phi/\partial z$ is the vertical component of the electric field, $\nabla_\perp$ denotes the gradient operator in the two dimensions transverse to **B**, $\boldsymbol{E}_\perp$ is the transverse electric field.

Let us represent the pre-earthquake perturbation in the vertical atmospheric field at the Earth's surface to be as follows (Hegai et al. 2015)

$$\Delta \boldsymbol{E}_z = \boldsymbol{E}(r) \sin \omega t \tag{14}$$

where

$$\boldsymbol{E}(r) = \boldsymbol{E}_0 \exp\,[\ln 10\,(r/R_0)^2] \tag{15}$$

where $\boldsymbol{E}_0$ and R_0 are, respectively, the peak value and the scale of the perturbation in the electric field. Assuming azimuthal symmetry, we can obtain from Eq. (11) and Eq. (12) the following equation describing the electrostatic potential Φ at altitudes from 0 to 90 km

$$\partial^2\Phi/\partial r^2 + (1/r)\,\partial\Phi/\partial r + (1/\sigma)\,\partial(\sigma\partial\Phi/\partial z)\partial z = 0 \tag{16}$$

Hence, Eq. (13) is explicitly expressed as

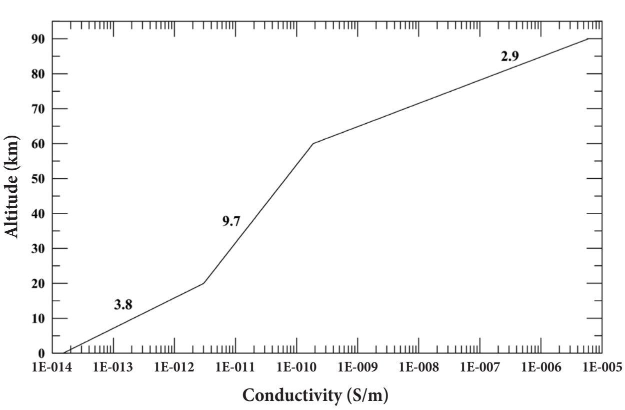

Fig. 1. Model altitude profile of the electrical conductivity of the atmosphere. The numbers next to the curves are scale heights in km.

$$\sigma\partial\Phi/\partial z = \Sigma_p\,(\partial^2\Phi/\partial r^2 + 1/r\,\partial\Phi/\partial r) \tag{17}$$

The adopted conductivity vertical profile is shown in Fig. 1. The profile is divided into three altitude sections (0-20 km, 20-60 km and 60-90 km), within each of which the conductivity is approximated by a simple exponential function of z as follows

$$\sigma_i = n_i \exp\{(z - z_i - 1)/h_i\} \quad (z_{i-1} \le z \le z_i) \tag{18}$$

where i =1, 2, 3, $n_1 = 1.5\ 10^{-14}$ S/m, $n_2 = n_1\exp\{(z_1 - z_0)/h_1\}$, $n_3 = n_2\exp\{(z_2 - z_1)/h_2\}$, z_0 = 0 km, z_1 = 20 km, z_2 = 60 km, z_3 = 90 km, h_1 = 3.8 km, h_2 = 9.7 km, h_3 = 2.9 km. This conductivity profile nearly fits the atmospheric conductivity model by Rycroft et al. (2007). Within each altitude section, the solution to Eq. (15) can be written in the form

$$\Phi = \int_0^\infty J_0(kr)[A_i(k)\exp(c_{1i}z) + B_i(k)\exp(c_{2i}z)]dk \tag{19}$$

where J_0 is the zero-order Bessel function of the first kind, A_i and B_i are coefficients determined from the boundary conditions, and $c_{1i} = -l/(2h_i) - [l/(2h_i)^2 + k^2]^{1/2}$, $c_{2i} = -l/(2h_i) + [l/(2h_i)^2 + k^2]^{1/2}$.

3. RESULTS AND DISCUSSION

To calculate the potential Φ at $z \ge 90$ km, Eq. (19) is subject to the following boundary conditions:

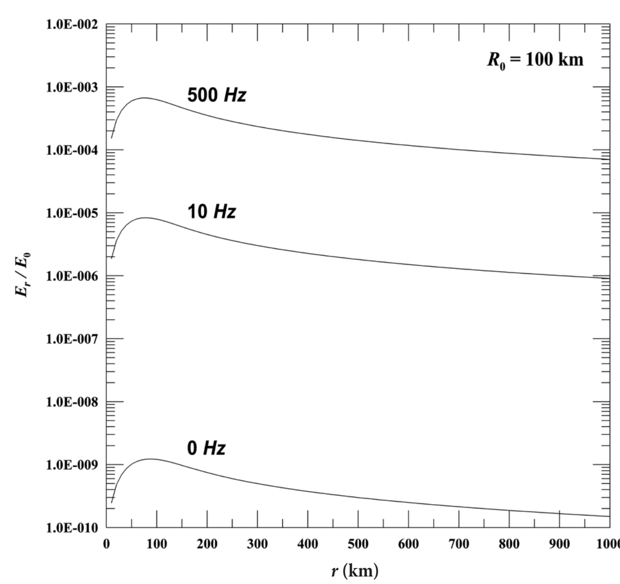

Fig. 2. Normalized horizontal electric field in the nighttime ionosphere at $z \ge 90$ km as a function of horizontal distance r for different values of the frequency of the seismogenic vertical Coulomb field on the Earth's surface and for the field scale size R_0 = 100 km.

1. $-\partial\Phi/\partial z = E_0 \exp[\ln 10\,(r/R_0)^2]$ at $z = z_b$
2. Φ is continuous at z = 20 and 60 km
3. $\sigma\,\partial\Phi/\partial z = \Sigma_p\,(\partial^2\Phi/\partial r^2 + 1/r\,\partial\Phi/\partial r)$ at z = 90 km

Fig. 2 shows an amplitude of the lateral electric field component $\boldsymbol{E}_r = -\partial\Phi/\partial r$ normalized to $|\boldsymbol{E}_0|$ as a function of r in the nighttime midlatitude ionosphere at $z \geq 90$ km for R_0 = 100 km and for three values of a linear frequency $f = \omega/2\pi$: 0, 10, and 500 Hz; the values of z_b corresponding to these frequencies are 0, 50, and 70 km, respectively. Solar minimum conditions are considered with Σ_p = 0.2 S at night. All three curves demonstrate similar behavior, attaining first a maximum at ~100 km and then revealing a gradual lowering, but the magnitude of the electric field depends sensitively on f. For E_0 = 30 V/m, the maximum E_r ~ 0.06, 0.55 and 20 mV/m for f = 0, 10, and 500 Hz, respectively. Note that the vector of the lateral electric field is $\boldsymbol{E}_r = (E_r \sin\omega t)\,\boldsymbol{e}_r$ where $\boldsymbol{e}_r$ is the radial unit vector.

Thus the time-varying perturbation in the vertical Coulomb field on the Earth's surface with a frequency of 500 Hz can produce at ionospheric heights the time-varying transverse electric field with amplitude of ~20 mV/m even when amplitude of the perturbation in the vertical electric field on the Earth's surface is as low as 30 V/m. In contrast, to produce the electric field of the same amplitude in the ionosphere, the time independent (f = 0) vertical electrostatic field on the Earth's surface with the peak magnitude by factor of ~7×10^5 larger would be required. The time-varying electric field of 20 mV/m amplitude produces significant Joule heating the nighttime F region ionospheric plasma inside a magnetic flux tube at the rate $Q = [(E_r)^2\,\Sigma_p]/2$. It can result in the excitation of acoustic gravity waves in the F region (Hegai et al. 1997, 2006) and in the reduction of the downward plasma flux from the protonosphere that plays an important role in the maintaining of the nighttime F2-layer. Both of these factors will produce modification of ionospheric plasma density. The reduction of the downward plasma flux will result in decreasing the main ionospheric plasma density peak N_mF2 over the earthquake's epicentral zone, while the excited acoustic gravity waves will produce perturbations in the F region plasma density several hundreds of kilometers far away from the earthquake's epicenter (Hegai et al. 2006).

It is noteworthy that for the adopted conductivity model, the 30 V/m perturbation in the vertical electric field on the Earth's surface is produced by a vertical electric current with a density of as small magnitude as ~4.5×10^{-13} A/m^2. We assume that the time-varying vertical electric current on the Earth's surface with such an amplitude could be generated prior an earthquake within the earthquake's epicentral zone due to some seismogenic micro-processes in the lithosphere. The calculated amplitude of the electric field penetrated into the ionosphere at 10 Hz is comparable to the magnitude of the ULF electric field at frequency of 15 Hz observed by DEMETER satellite before earthquakes in the ionosphere at 660-710 km (Huang et al. 2014) if E_0 = 300 V/m. Our formalism is valid for frequencies of the seismogenic vertical electric field less than 1,000 Hz. In this case, the half-length of electromagnetic wave is 150 km that larger than the distance between the ground and the lower boundary of the ionosphere and therefore, it allows us to ignore wavy properties of the seismogenic electric field when studying its penetration into the ionosphere.

It should be noted that the seismogenic perturbation in the time-varying vertical Coulomb electric field at 500 Hz with as short duration as ~15 min will produce much longer perturbations in the F region electron density via a reduction in the downward plasma flux and excited acoustic gravity waves (Hegai et al. 2006), lasting for 2-3 hours. This temporal "widening" of the ionospheric effect is important from the observational point of view because a short pulse of the pre-earthquake seismogenic electric field is difficult to detect on the Earth's surface and by a satellite in the ionosphere. The results above clearly indicate that the altitude dependence of the atmospheric conductivity provides the most favorable opportunity for effective penetration into the ionosphere for the Fourier components of the seismogenic vertical Coulomb field perturbation on the Earth's surface with frequencies of several hundred Hz while electric fields at lower frequencies penetrate in the ionosphere much weaker, i.e., the lower atmosphere plays a role of some frequency dependent filter that strongly controls a penetration of Coulomb electric fields of various frequencies from the ground up to the ionosphere.

4. CONCLUSION

It can be concluded that a time-varying Coulomb vertical electric field at a frequency of 500 Hz, presumably generated on the Earth's surface before an earthquake within its epicentral zone, efficiently penetrates into the nighttime ionosphere of high and middle latitudes and can produce measurable perturbations in the F region electron density via significant Joule heating of the F region plasma resulting in a reduction of a downward plasma flux from the protonosphere and in an excitation of acoustic gravity waves. The time-varying Coulomb vertical electric field with a frequency of 500 Hz is mapped from the ground into the ionosphere by a factor of ~7×10^5 more efficient than a time independent Coulomb vertical electric field. Even a short (~15 min) pulse of the seismogenic time-varying Coulomb vertical electric field can cause perturbations in the F region electron density for the period of 2-3 hours.

ACKNOWLEDGMENTS

This work was supported by the research grant of Russian Academy of Sciences.

REFERENCES

Artru J, Farges T, Lognonné P, Acoustic waves generated from seismic surface waves: propagation properties determined from Doppler sounding observations and normal-mode modelling, Geophys. J. Int. 158, 1067-1077 (2004). https://doi.org/10.1111/j.1365-246X.2004.02377.x

Astafyeva EI, Afraimovich EL, Long-distance traveling ionospheric disturbances caused by the great Sumatra-Andaman earthquake on 26 December 2004, Earth Planets Space 58, 1025-1031 (2006). https://doi.org/10.1186/BF03352607

Calais E, Minster JB, GPS detection of ionospheric perturbations following the January 17, 1994, Northridge earthquake, Geophys. Res. Lett. 22, 1045-1048 (1995). https://doi.org/10.1029/95GL00168

Daneshvar MRM, Freund FT, Remote sensing of atmospheric and ionospheric signals prior to the M_w 8.3 Illapel earthquake, Chile 2015, Pure Appl. Geophys. 174, 11-45 (2017). https://doi.org/10.1007/s00024-016-1366-0

Ducic V, Artru J, Lognonné P, Ionospheric remote sensing of the Denali earthquake Rayleigh surface waves, Geophys. Res. Lett. 30, 1951 (2003). https://doi.org/10.1029/2003GL017812

Hao J, Tang TM, Li DR, Progress in the research of atmospheric electric field anomaly as an index for short-impending prediction of earthquakes, J. Earthq. Pred. Res. 8, 241-255 (2000).

Hegai VV, Kim VP, Nikiforova LI, A possible generation mechanism of acoustic-gravity waves in the ionosphere before strong earthquakes, J. Earthq. Pred. Res. 6, 584-589 (1997).

Hegai VV, Kim VP, Liu JY, The ionospheric effect of atmospheric gravity waves excited prior to strong earthquake, Adv. Space Res. 37, 653-659 (2006). https://doi.org/10.1016/j.asr.2004.12.049

Hegai VV, Kim VP, Liu JY, On a possible seismomagnetic effect in the topside ionosphere, Adv. Space Res. 56, 1707-1713 (2015). https://doi.org/10.1016/j.asr.2015.07.034

Hegai VV, Kim VP, Legen'ka AD, Ionospheric F2-layer perturbations observed after the M8.8 Chile earthquake on February 27, 2010, at long distance from the epicenter, J. Astron. Space Sci. 34, 1-5 (2017). https://doi.org/10.5140/JASS.2017.34.1.1

Huang CC, Liu JYG, Seismo-ionospheric anomalies in DEMETER observations during the Wenchuan M7.9 earthquake, in 2014 AGU Fall Meeting, San Francisco, CA, 15-19 Dec 2014.

Kelley MC, Swartz WE, Heki K, Apparent ionospheric total electron content variations prior to major earthquakes due to electric fields created by tectonic stresses, J. Geophys. Res. 122, 6689-6695 (2017). https://doi.org/10.1002/2016JA023601

Kim VP, Hegai VV, On the variability of the ionospheric F2-layer during the quietest days in December 2009, J. Astron. Space Sci. 33, 273-278 (2016). https://doi.org/10.5140/JASS.2016.33.4.273

Kim VP, Liu JY, Hegai VV, Modeling the pre-earthquake electrostatic effect on the F region ionosphere, Adv. Space Res. 50, 1524-1533 (2012). https://doi.org/10.1016/j.asr.2012.07.023

Kuo CL, Huba JD, Joyce G, Lee LC, Ionosphere plasma bubbles and density variations induced by pre-earthquake rock currents and associated surface charges, J. Geophys. Res. 116, A10317 (2011). https://doi.org/10.1029/2011ja016628

Kuo CL, Lee LC, Huba JD, An improved coupling model for the lithosphere-atmosphere-ionosphere system, J. Geophys. Res. 119, 3189-3205 (2014). https://doi.org/10.1002/2013JA019392

Leonard RS, Barnes Jr. RA, Observation of ionospheric disturbances following the Alaska earthquake, J. Geophys. Res. 70, 1250-1253 (1965). https://doi.org/10.1029/JZ070i005p01250

Li M, Parrot M, Statistical analysis of an ionospheric parameter as a base for earthquake prediction, J. Geophys. Res. 118, 3731-3739 (2013). https://doi.org/10.1002/jgra.50313

Liu HF, Ding B, Zhao J, Li L, Hu L, et al., Ionospheric response following the M_w 7.8 Gorkha earthquake on 25 April 2015, J. Geophys. Res. 122, 6495-6507 (2017). https://doi.org/10.1002/2016JA023079

Liu JY, Chen YI, Chuo YJ, Chen CS, A statistical investigation of preearthquake ionospheric anomaly, J. Geophys. Res. 111, A05304 (2006). https://doi.org/10.1029/2005JA011333

Liu JY, Chen YI , Chen CH, Hattori K, Temporal and spatial precursors in the ionospheric Global Positioning System (GPS) total electron content observed before the 26 December 2004 M9.3 Sumatra–Andaman earthquake, J. Geophys. Res. 115, A09312 (2010). https://doi.org/10.1029/2010JA015313

Liu JY, Le H , Chen YI, Chen CH, Liu L, et al., Observations and simulations of seismoionospheric GPS total electron content anomalies before the 12 January 2010 *M7* Haiti earthquake, J. Geophys. Res. 116, A04302 (2011). https://doi.org/10.1029/2010JA015704

Maruyama T, Yusupov K, Akchurin A, Ionosonde tracking of infrasound wavefronts in the thermosphere launched by seismic waves after the 2010 M8.8 Chile earthquake, J. Geophys. Res. 121, 2683-2692 (2016). https://doi.org/10.1002/2015JA022260

Oyama KI, Kakinami Y, Liu JY, Kamogawa M, Kodama T, Reduction of electron temperature in low latitude ionosphere at 600 km before and after large earthquakes, J. Geophys. Res. 113, A11317 (2008). https://doi.org/10.1029/2008JA013367

Oyama KI, Kakinami Y, Liu JY, Abdu MA, Cheng CZ, Latitudinal distribution of anomalous ion density as a precursor of a large earthquake, J. Geophys. Res. 116, A04319 (2011). https://doi.org/10.1029/2010JA015948

Pulinets S, Boyarchuk K, Ionospheric Precursors of Earthquakes (Springer, Berlin, 2004).

Rishbeth H, Day-to-day ionospheric variations in a period of high solar activity, J. Atmos. Terr. Phys. 55, 165-171 (1993). https://doi.org/10.1016/0021-9169(93)90121-E

Rishbeth H, Mendillo M, Patterns of F2-layter variability, J. Atmos. Sol.-Terr. Phys. 63, 1661-1680 (2001). https://doi.org/10.1016/S1364-6826(01)00036-0

Rolland LM, Lognonné P, Munekane H, Detection and modeling of Rayleigh wave induced patterns in the ionosphere, J. Geophys. Res. 116 A05320 (2011). https://doi.org/10.1029/2010JA016060

Row RV, Evidence of long-period acoustic-gravity waves launched into the F region by the Alaskan earthquake of March 28, 1964, J. Geophys. Res. 71, 343-345 (1966). https://doi.org/10.1029/JZ071i001p00343

Rycroft MJ, Odzimek A, Arnold NF, Füllekrug M, Kulak A, et.al., New model simulations of the global atmospheric electric circuit driven by thunderstorms and electrified shower clouds: The roles of lightning and sprites, J. Atmos. Sol.-Terr. Phys. 69, 2485-2509 (2007).

Zhang X, Shen X, Parrot M, Zeren Z, Ouyang X, et al., Phenomena of electrostatic perturbations before strong earthquakes (2005–2010) observed on DEMETER, Nat. Hazards Earth Syst. Sci. 12, 75-83 (2012). https://doi.org/10.5194/nhess-12-75-2012

Zhang X, Shen X, Zhao S, Yao L, Quyang X, et al., The characteristics of quasistatic electric field perturbations observed by DEMETER satellite before large earthquakes, Journal of Asian Earth Sciences 79, 42–52 (2014). https://doi.org/10.1016/j.jseaes.2013.08.026

Zhao B, Wang M, Yu T, Wan W, Lei J, et al., Is an unusual large enhancement of ionospheric electron density linked with the 2008 great Wenchuan earthquake?, J. Geophys. Res. 113, A11304 (2008). https://doi.org/10.1029/2008JA013613